

• Supplementary File •

# Leaderless output sign consensus of heterogeneous multi-agent systems over switching signed graphs

Yihan MENG<sup>1</sup>, Hongwei ZHANG<sup>1\*</sup> & Aiguo WU<sup>1</sup>

<sup>1</sup>*School of Mechanical Engineering and Automation, Harbin Institute of Technology, Shenzhen 518055, China*

## Appendix A Literature review

In recent years, distributed control of multi-agent systems (MASs) has drawn great interest due to its wide applications in power systems [1], transportation systems [2] and vehicle formation [3], to just name a few. Productive results have been obtained, with most of them centering on MASs over cooperative relationships [4–6]. To put it in another way, the communication graph, in which nodes and edges represent agents and interaction links, respectively, are considered to be non-negative [7].

In practice, however, antagonistic and cooperative relations coexist within many MASs, such as social networks [8], financial markets [9] and brain networks [10]. When encountering antagonistic interactions, one resorts to signed graphs, where positive edges stand for cooperative interactions and negative edges stand for antagonistic interactions. Compared with non-negative graphs, signed graphs better characterize the co-opetitive relations among all agents. The investigation of signed graphs is generally challenging, since the traditional definition of Laplacian matrix for non-negative graphs, along with all its properties are no longer suitable for signed graphs.

Most research works about MASs over non-negative graphs focus on consensus behavior of MASs, whereas the collective behaviors displayed over signed graphs are more convoluted, and needs further investigation. One such behavior, called bipartite consensus [11], arises from structurally balanced signed graphs [12]. Specifically, over a structurally balanced signed graph, all agents in a MAS are divided into two subgroups, where agents within the same subgroup are collaboratively related while agents from distinct subgroups have antagonistic interactions. With appropriate control protocol, the output signals of agents from two different subgroups will eventually have the same magnitude but opposite signs [11, 13–15]. Nonetheless, it is rather hard for a signed graph to satisfy the condition of being structurally balanced, since a simple alteration of the signs of some edges, as well as an addition or a deletion of certain edges would break such balance. Furthermore, without the graph being structurally balanced, techniques that transform the signed graphs into non-negative graphs are no longer applicable, and therefore, how MASs behave over structurally unbalanced signed graphs is a challenging problem and deserves further investigation. By utilizing Perron-Frobenius property [16], researchers unveiled that MASs over a certain sub-class of structurally unbalanced graphs, called eventually positive signed graphs [17], are able to perform a collective behavior called unanimity of opinions [18], such unanimity is manifested by the same sign of the output signals at the same time, and is also known as sign consensus [19]. This synchronous behavior has huge potential for applications in the area of opinion dynamics. For example, in the study of dynamic behavior of social networks with state-dependent susceptibility [20], the agents of the network, under the stubborn extremists scenario, eventually achieve a unanimous opinion. Works on sign consensus is now enriched with homogeneous [19] and heterogeneous [21] MASs, MASs over fixed [19] and switching [22] topologies. In several recent works [21, 23], output sign consensus of heterogeneous MASs is achieved over eventually positive signed graphs. While in both works, the existence of a practical leadership is assumed to be a mandatory condition. It is also worth mentioning that for heterogeneous MASs, most current works adopt a leader-follower scheme to achieve a synchronous behavior [24, 25].

However, practically speaking, a group can be leaderless. As in the research of animal navigation [26], the “Many-wrongs principle” assumes that all individuals have a similar amount of information, and the pooling of the information in the animal group leads to accurate navigation. In this sense, this animal navigation mechanism is largely dependent on the information that individuals can provide, rather than being led by a leader. Thus, how to manage leaderless MASs needs investigation. Recently, a work studying leaderless heterogeneous multiple Euler-Lagrange systems proposed a distributed “observer” method to solve consensus problem of a leaderless MAS [27]. Specifically, a distributed “observer” is proposed for the multiple Euler-Lagrange system such that all “observers” eventually reach consensus about a constant system matrix and a common trajectory, then based on internal model principle and adaptive regulation, the MAS reaches state consensus. Moreover, our latest work studied output sign consensus of heterogeneous MASs over signed graphs, where there is no leader node [28].

Notice that the majority of studies on MASs considers the communication network to be fixed, while in many practical scenarios, the network can be dynamically changing. For example, the social networks among human beings are often dynamic. People respond to cooperation and competition of people around them by making or breaking network links [29]. In addition, considering that the communication graph is always time-varying, the assumption that the signed graph is fixed and eventually positive, along with all the properties such graphs bring cease to apply. Hence, leaderless output sign consensus (LOSC) of heterogeneous MASs over switching signed digraphs is challenging and needs further study.

## Appendix B Notations

The notations used in this study are rather standard.  $\|\cdot\|$  denotes the Euclidian norm.  $\mathbb{R}$  is the set of all real numbers, and  $\mathbb{R}^+$  is the set of all positive real numbers.  $\otimes$  denotes the Kronecker product.  $\text{col}(X_1, X_2, \dots, X_N) = [X_1^T, X_2^T, \dots, X_N^T]^T \in \mathbb{R}^{N \times n}$ ,  $\forall X_i \in \mathbb{R}^{m \times n}$ , and  $\text{vec}(X) = \text{col}(X_1, X_2, \dots, X_n)$ , where  $X_i \in \mathbb{R}^m$  is the  $i$ -th column of matrix  $X \in \mathbb{R}^{m \times n}$ . For matrix  $A = [a_{ij}]$ ,

\* Corresponding author (email: hwzhang@hit.edu.cn)

$a_{ij}$  is the entry at the  $i$ th row and  $j$ th column.  $A \succ 0$  means  $A$  is an entrywise positive matrix, i.e. for all  $i, j$ ,  $a_{ij} > 0$ , and  $v \succ 0$  is defined similarly.  $A > 0$  means  $A$  is a positive definite symmetric matrix. Expression  $\Lambda = \text{diag}(\lambda_1, \lambda_2, \dots, \lambda_N)$  constructs a diagonal matrix  $\Lambda$  in which the diagonal entries are  $\lambda_i$ .  $\rho(A)$  is the spectral radius of matrix  $A \in \mathbb{R}^{n \times n}$ .  $\lambda_i(A)$  is the  $i$ th eigenvalue of matrix  $A$ .  $\min(k_i)$  gives the minimum of the sequence  $\{k_i\}$ .  $\text{Re}(\lambda)$  means the real part of a complex number  $\lambda$ . Function  $M_m^q(\cdot)$  is defined such that for a vector  $x = \text{col}(x_1, x_2, \dots, x_q) \in \mathbb{R}^{qm}$ , where  $x_i \in \mathbb{R}^m$ ,  $M_m^q(x) = [x_1, x_2, \dots, x_q] \in \mathbb{R}^{m \times q}$ . The signum function  $\text{sgn}(\cdot)$  is defined such that for a vector  $x = [x_1, x_2, \dots, x_m]^T \in \mathbb{R}^m$ ,  $\text{sgn}(x) = [\text{sgn}(x_1), \text{sgn}(x_2), \dots, \text{sgn}(x_m)]^T$ , where

$$\text{sgn}(x_i) = \begin{cases} 1, & x_i > 0, \\ 0, & x_i = 0, \\ -1, & x_i < 0, \end{cases}$$

$\text{sgn}(\cdot)$  is similarly defined for a real matrix  $A \in \mathbb{R}^{m \times n}$ .

## Appendix C Graph theory and preliminaries

A digraph is used to describe the communication network of a MAS, where an agent is represented by a node, and the interaction between two neighboring agents is represented by an edge between the two nodes. A digraph is denoted by  $\mathcal{G} = (\Omega, \mathcal{E})$ , where  $\Omega = \{1, 2, \dots, N\}$  is the node set, and  $\mathcal{E} \subset \Omega \times \Omega$  is the edge set. The topology of a digraph is captured by an adjacency matrix  $\mathcal{A} = [a_{ij}] \in \mathbb{R}^{N \times N}$ ,  $a_{ij} \neq 0$  if and only if  $(j, i) \in \mathcal{E}$ , which indicates that information flows from node  $j$  to node  $i$ , and node  $j$  is a neighboring node of node  $i$ ; otherwise  $a_{ij} = 0$ .  $\mathcal{N}_i = \{j \mid (j, i) \in \mathcal{E}\}$  is the index set of all neighbors of node  $i$ . In this study, no self-loop is contained in the graph, i.e.  $a_{ii} = 0, \forall i$ .  $\mathcal{G}(\mathcal{A})$  is non-negative if and only if  $a_{ij} \geq 0, \forall i, j$  and is a signed graph otherwise.

For switching graphs, we consider a sequence of bounded and non-overlapping switching time intervals  $[t_k, t_{k+1}), k \in \{0, 1, 2, \dots\}$ , such that  $t_0 = 0$  and  $\lim_{k \rightarrow \infty} t_k = \infty$ . Divide each interval into  $m_k$  sub-intervals  $[t_{k_0}, t_{k_1}), [t_{k_1}, t_{k_2}), \dots, [t_{k_{m_k-1}}, t_{k_{m_k}})$ , where  $t_{k_0} = t_k$  and  $t_{k_{m_k}} = t_{k+1}$ . The topology of a switching signed graph  $\mathcal{G}(\mathcal{A}_{\delta(t)})$ , where  $\delta(t) : [t_k, t_{k+1}) \rightarrow \{k_0, k_1, \dots, k_{m_k-1}\}$  is the switching signal, is assumed to be fixed in each sub-interval. We also define dwell time  $\tau_{k_i} = t_{k_{i+1}} - t_{k_i}, i = 0, 1, \dots, m_k - 1$ .

**Definition 1** (Eventually Positive). [17] If there exists a positive integer  $k_0$  such that for all integer  $k \geq k_0$ , the  $k$ th power of a matrix  $A \in \mathbb{R}^{n \times n}$  is positive entrywise, i.e.,  $A^k \succ 0$ , then matrix  $A$  is eventually positive.

**Definition 2** (Jointly Eventually Positive). [23] A switching signed graph  $\mathcal{G}(\mathcal{A}_{\delta(t)})$  is said to be jointly eventually positive, if there exists a sequence of bounded and non-overlapping switching time intervals  $[t_k, t_{k+1}), k \in \{0, 1, 2, \dots\}$ , such that

$$\bar{A} = \int_{t_k}^{t_{k+1}} \mathcal{A}_{\delta(t)} dt$$

is eventually positive,  $\forall k \in \{0, 1, 2, \dots\}$ .

**Definition 3.** [16] For a matrix  $A \in \mathbb{R}^{n \times n}$ , if the spectral radius  $\rho(A)$  is a simple eigenvalue, and the corresponding right eigenvector  $v_r$  is positive entrywise, i.e.,  $v_r \succ 0$ , then  $A$  is said to possess strong Perron-Frobenius property.

**Proposition 1.** [16] Consider a matrix  $A \in \mathbb{R}^{n \times n}$ , the following three statements are equivalent:

1.  $A$  is an eventually positive matrix;
2.  $A^T$  is an eventually positive matrix;
3. Matrices  $A$  and  $A^T$  possess strong Perron-Frobenius property.

## Appendix D Technical lemmas

**Lemma 1.** [30] Consider the following system

$$\dot{x}(t) = f(x, \alpha t) \tag{D1}$$

with  $f : W \times \mathbb{R} \rightarrow \mathbb{R}^n$ , where  $W \subset \mathbb{R}^n$  is open,  $0 \in W$  and  $f(0, t) = 0, \forall t \in \mathbb{R}$ . There exists a constant  $\alpha^* > 0$  such that for all  $\alpha > \alpha^*$ , (D1) has an exponentially stable equilibrium point  $x = 0$  if the following two conditions are satisfied:

1. There exists a Lyapunov function  $V(x)$  and strictly positive numbers  $\lambda_{min}$  and  $\lambda_{max}$  such that for all  $x \in U (U \subset W$  and  $U$  is open and  $0 \in U)$ ,  $\lambda_{min} x^T x \leq V(x) \leq \lambda_{max} x^T x$ . In addition,  $\frac{\partial V}{\partial x}(0) = 0$  and  $\frac{\partial V}{\partial x}(x)$  is Lipschitz on  $U$  with Lipschitz constant  $K_v$ ;
2. There exists an increasing sequence of times  $t_k (k \in \{0, 1, 2, \dots\})$  with  $t_k \rightarrow \infty$  as  $k \rightarrow \infty$ , and exists  $T > 0$  such that  $t_{k+1} - t_k \leq T$  and  $v > 0$  such that  $\forall t_k$  and  $\forall x \in U$

$$\frac{\partial V}{\partial x}(x) \int_{t_k}^{t_{k+1}} f(x, \tau) d\tau \leq -v \|x\|^2.$$

Elaborate Lemma 1 into linear cases, we obtain the following result:

**Lemma 2.** [30] Consider a linear time-varying(LTV) system

$$\dot{x}(t) = A(t)x(t),$$

where  $A(t) : \mathbb{R} \rightarrow \mathbb{R}^{n \times n}$ . If there exists an infinite increasing sequence of time instants  $\{t_k\}, k \in \{0, 1, 2, \dots\}$ , with  $t_0 \geq 0$ ,  $\lim_{k \rightarrow \infty} t_k = \infty$ , and  $t_{k+1} - t_k \leq T$  for some positive  $T$ , such that its average systems

$$\dot{\bar{x}}(t) = \frac{\int_{t_k}^{t_{k+1}} A(t) dt}{t_{k+1} - t_k} \bar{x}(t), k \in \{0, 1, 2, \dots\}$$

are exponentially stable, then  $\exists \alpha^* > 0$  such that  $\forall \alpha > \alpha^*$ , the fast time-varying system

$$\dot{x}(t) = A(\alpha t)x(t)$$

is exponentially stable.

According to Remark 4 in [30],  $\alpha^*$  can be computed by

$$e^{\frac{KT}{\alpha^*}} \frac{T}{\alpha^*} = \frac{1}{K} \left( \sqrt{1 + \frac{v}{K_v KT}} - 1 \right), \quad (D2)$$

where  $K$  is the maximum of the upper bounds of the Lipschitz function  $l_x(t)$  of  $f(x, t)$ ,  $K_v$  is the Lipschitz constant of  $\frac{\partial V}{\partial x}(x)$ , and  $v$  is a positive constant defined in the second condition of Lemma 1. From (D2), we can see that if  $T$  is small enough,  $\alpha^*$  can be less than one, and thus, we choose  $\alpha > \alpha^*$  to be one.

**Lemma 3.** [22] For any matrix  $A \in \mathbb{R}^{N \times N}$  and a vector  $v = [v_1, \dots, v_N]^T \succ 0$ , there exists a diagonal matrix  $\Sigma = \text{diag}(\sigma_1, \dots, \sigma_N) \in \mathbb{R}^{N \times N}$  such that  $(\Sigma - A)v = 0$ , and matrix  $L = \Sigma - A$  can be decomposed as  $L = ME$  where  $M \in \mathbb{R}^{N \times (N-1)}$ ,

$$E = \begin{bmatrix} \frac{1}{v_1} & -\frac{1}{v_2} & 0 & \cdots & 0 \\ 0 & \frac{1}{v_2} & -\frac{1}{v_3} & \cdots & 0 \\ \vdots & \vdots & \ddots & \ddots & \vdots \\ 0 & 0 & \cdots & \frac{1}{v_{N-1}} & -\frac{1}{v_N} \end{bmatrix} \quad (D3)$$

and  $E \in \mathbb{R}^{(N-1) \times N}$ . If  $A$  is eventually positive and  $v$  is the eigenvector corresponding to  $\rho(A)$ , then  $M$  is of full column rank and  $\text{Re}(\lambda_i(EM)) > 0$ ,  $\forall i$ .

We propose the following lemma which facilitates the development of the distributed ‘‘sign observer’’.

**Lemma 4.** Consider the following system:

$$\dot{x} = F(t)x + G(t),$$

where  $x \in \mathbb{R}^n$ ,  $F(\cdot) : \mathbb{R} \rightarrow \mathbb{R}^{n \times n}$ ,  $G(\cdot) : \mathbb{R} \rightarrow \mathbb{R}^n$ , and  $F(t)$  and  $G(t)$  are bounded and piecewise continuous. Then  $x$  converges to a bounded vector, if both  $F(t)$  and  $G(t)$  vanish exponentially.

*Proof.* Consider a Lyapunov function candidate  $V = x^T x$ . Take the time derivative of  $V$  as:

$$\dot{V} = x^T \left( F^T(t) + F(t) \right) x + 2G^T(t)x.$$

Since both  $F(t)$  and  $G(t)$  decay to 0 exponentially, there exist positive constants  $\alpha$ ,  $\beta$ ,  $\lambda$  and  $\gamma$  such that  $\|F(t)\| \leq \alpha e^{-\lambda t}$  and  $\|G(t)\| \leq \beta e^{-\gamma t}$ . Notice that  $G^T(t)x \leq \|G(t)\| \|x(t)\|$ . Then we have

$$\dot{V} \leq 2\alpha e^{-\lambda t} \|x\|^2 + 2\beta e^{-\gamma t} \|x\|.$$

Let  $W = \sqrt{V} = \|x(t)\|$ . Taking the time derivative of  $W$  gives

$$\dot{W} = \frac{\dot{V}}{2\sqrt{V}} \leq \alpha e^{-\lambda t} W + \beta e^{-\gamma t}$$

Then  $\forall t \geq 0$ ,

$$\begin{aligned} W &\leq e^{\int_0^t \alpha e^{-\lambda \tau} d\tau} \|x(0)\| + \int_0^t e^{\int_0^\tau \alpha e^{-\lambda s} ds} \beta e^{-\gamma \tau} d\tau \\ &= \frac{\alpha}{\lambda} \left( 1 - e^{-\lambda t} \right) \|x(0)\| + \beta \int_0^t e^{\frac{\alpha}{\lambda} (1 - e^{-\lambda \tau}) - \gamma \tau} d\tau \\ &\leq \frac{\alpha}{\lambda} \|x(0)\| + \beta e^{\frac{\alpha}{\lambda}} \int_0^t e^{-\gamma \tau} d\tau \\ &\leq \frac{\alpha}{\lambda} \|x(0)\| + \frac{\beta}{\gamma} e^{\frac{\alpha}{\lambda}}, \end{aligned}$$

which implies that  $\|x(t)\|$  eventually converges to a bounded vector for all  $x(0)$  and  $t \geq 0$ .

The following output regulation-related lemma is provided for the design of the controllers.

**Lemma 5.** [21] Consider the following systems

$$\dot{\chi}_i = -\mu_3 Q_i^T(t) [Q_i(t)\chi_i - d_i], \quad \forall i \quad (D4)$$

where

$$d_i = \text{vec} \left( \begin{bmatrix} 0_{n_i \times p} \\ -I_p \end{bmatrix} \right), \quad Q_i(t) = S_i^T(t) \otimes \begin{bmatrix} I_{n_i} & 0 \\ 0 & 0 \end{bmatrix} - I_p \otimes \begin{bmatrix} v_{r_i} A_i & B_i \\ C_i & 0 \end{bmatrix}$$

and  $\mu_3$  is large enough. Let

$$Q_i = v_{r_i} (S^*)^T \otimes \begin{bmatrix} I_{n_i} & 0 \\ 0 & 0 \end{bmatrix} - I_p \otimes \begin{bmatrix} v_{r_i} A_i & B_i \\ C_i & 0 \end{bmatrix}.$$

If the following regulator equations

$$\begin{aligned} v_{r_i} \Pi_i S^* &= v_{r_i} A_i \Pi_i + B_i \Gamma_i \\ C_i \Pi_i &= I_p, \end{aligned} \quad (D5)$$

can be solved, and  $\text{rank}(Q_i) = \text{rank}([Q_i, d_i])$ , then for any initial conditions  $\chi_i(t_0)$ ,  $\chi_i(t)$  exists and has a unique solution. Rearrange  $\chi_i$  as follows:

$$\Upsilon_i(t) = M_{n_i + m_i}^p(\chi_i(t)) = \text{col}(\Upsilon_{1i}(t), \Upsilon_{2i}(t)), \quad (D6)$$

we have that  $\Upsilon_i(t)$  approaches  $\text{col}(\Pi_i, \Gamma_i)$  exponentially as  $t \rightarrow \infty$  with  $\mu_3 > \frac{\omega}{\kappa}$ , where  $\omega$  is the rate at which  $S_i(t)$  converges to  $v_{r_i} S^*$  and  $\kappa$  is the minimal nonzero singular value of  $Q_i$ .

## Appendix E Distributed “sign observer”

This study solves LOSC problem by utilizing a distributed “sign observer”, so that the dynamics and the states of the virtual leader can be observed. The distributed “sign observer” is defined as follows:

**Definition 4** (Distributed “Sign Observer”). [28] Consider the following dynamics

$$\dot{\omega}_i = g_i(\omega_i, \omega_j |_{j \in \mathcal{N}_i}), \quad (\text{E1a})$$

$$i_i = h_i(\omega_i, \iota_i, \iota_j |_{j \in \mathcal{N}_i}). \quad (\text{E1b})$$

If there exists a graph  $\mathcal{G}$ , functions  $g_i(\cdot)$  and  $h_i(\cdot)$ , such that for arbitrary initial conditions  $\omega_i(0) \in \mathbb{R}^{m \times m}$  and  $\iota_i(0) \in \mathbb{R}^m$ , we have that  $\forall i, j$ ,

$$\lim_{t \rightarrow \infty} [\text{sgn}(\omega_i(t)) - \text{sgn}(\omega_j(t))] = 0 \text{ and } \lim_{t \rightarrow \infty} [\text{sgn}(\iota_i(t)) - \text{sgn}(\iota_j(t))] = 0.$$

Then (E1) is called a distributed “sign observer” for the leaderless MAS.

The concept of distributed “sign observer” was used for fixed topology cases [28], in which, without a prescribed practical leader, (E1) is able to observe the sign of an auto-system induced by the communication network and the initial state of the MAS. Whereas for switching topology cases, beside the graph topology and the agents’ initial conditions, the construction of the virtual leader further incorporates the influence from the nature of the “observer”. Dynamics (2) in the main article is the specific design of the distributed “sign observer” for this study.

The following lemma shows sign consensus of “sign observer” (2a):

**Lemma 6.** Consider “sign observer” (2a). If Assumption 1 holds, then for any positive scalar  $\mu_1$  and any initial conditions  $S_i(0)$ ,  $S_i(t)$  achieves sign consensus.

*Proof.* With  $\sigma_i(t) = \frac{\sum_{j=1}^N a_{ij}(t)v_{rj}}{v_{ri}}$ ,  $\Sigma_{\delta(t)} = \text{diag}(\sigma_1(t), \dots, \sigma_N(t))$  and  $L_{\delta(t)} = \Sigma_{\delta(t)} - \mathcal{A}_{\delta(t)}$ , straightforward computation gives

$$L_{\delta(t)}v_r = (\Sigma_{\delta(t)} - \mathcal{A}_{\delta(t)})v_r = 0. \quad (\text{E2})$$

Note that for matrix  $\bar{\mathcal{A}}$ , there exists a constant nonsingular matrix  $U$  such that  $U^{-1}\bar{\mathcal{A}}U = \mathcal{J}_{\bar{\mathcal{A}}}$ , where  $\mathcal{J}_{\bar{\mathcal{A}}}$  is the Jordan canonical

form of  $\bar{\mathcal{A}}$ . Let  $U = [v_r \ v_{N-1}]$ ,  $U^{-1} = \begin{bmatrix} u_l \\ u_{N-1} \end{bmatrix}$ , where  $v_{N-1} \in \mathbb{R}^{N \times (N-1)}$  contains the rest  $N-1$  columns of matrix  $U$ ,  $u_l \in \mathbb{R}^{1 \times N}$  is the first row of  $U^{-1}$  and  $u_{N-1} \in \mathbb{R}^{(N-1) \times N}$  contains the last  $N-1$  rows of  $U^{-1}$ . Introduce transformation  $\Phi = (U^{-1} \otimes I_p)S$ . Taking the time derivative of  $\Phi$  gives

$$\begin{aligned} \dot{\Phi} &= -\mu_1 \left( U^{-1} L_{\delta(t)} U \otimes I_p \right) \Phi \\ &= -\mu_1 \left( \begin{bmatrix} u_l \\ u_{N-1} \end{bmatrix} L_{\delta(t)} [v_r \ v_{N-1}] \otimes I_p \right) \Phi \\ &= -\mu_1 \left( \begin{bmatrix} 0 & l_{\delta(t)} \\ 0_{(N-1) \times 1} & L_{\delta(t)}^* \end{bmatrix} \otimes I_p \right) \Phi \end{aligned} \quad (\text{E3})$$

where  $l_{\delta(t)} = u_l L_{\delta(t)} v_{N-1} \in \mathbb{R}^{1 \times (N-1)}$  and  $L_{\delta(t)}^* = u_{N-1} L_{\delta(t)} v_{N-1} \in \mathbb{R}^{(N-1) \times (N-1)}$ . By integrating  $U^{-1} L_{\delta(t)} U$  within time interval  $[t_k, t_{k+1}]$ , one obtains

$$\begin{aligned} \int_{t_k}^{t_{k+1}} U^{-1} L_{\delta(t)} U dt &= \int_{t_k}^{t_{k+1}} \begin{bmatrix} 0 & l_{\delta(t)} \\ 0_{(N-1) \times 1} & L_{\delta(t)}^* \end{bmatrix} dt \\ &= \begin{bmatrix} 0 & \int_{t_k}^{t_{k+1}} l_{\delta(t)} dt \\ 0_{(N-1) \times 1} & \int_{t_k}^{t_{k+1}} L_{\delta(t)}^* dt \end{bmatrix}. \end{aligned} \quad (\text{E4})$$

On the other hand, (E2) implies  $\int_{t_k}^{t_{k+1}} (\Sigma_{\delta(t)} - \mathcal{A}_{\delta(t)})v_r dt = 0$ . It is trivial to show that

$$\int_{t_k}^{t_{k+1}} \Sigma_{\delta(t)} v_r dt = \int_{t_k}^{t_{k+1}} \mathcal{A}_{\delta(t)} v_r dt = \bar{\mathcal{A}} v_r = \rho(\bar{\mathcal{A}}) v_r,$$

which indicates that  $\int_{t_k}^{t_{k+1}} \Sigma_{\delta(t)} dt = \rho(\bar{\mathcal{A}}) I_N$ . Let  $\mathcal{J}_{\bar{\mathcal{A}}} = \text{diag}(\rho(\bar{\mathcal{A}}), \mathcal{J}_{\bar{\mathcal{A}}_{N-1}})$ , where  $\mathcal{J}_{\bar{\mathcal{A}}_{N-1}} \in \mathbb{R}^{(N-1) \times (N-1)}$  contains the last  $(N-1)$  columns and rows of  $\mathcal{J}_{\bar{\mathcal{A}}}$ . Then

$$\begin{aligned} \int_{t_k}^{t_{k+1}} U^{-1} L_{\delta(t)} U dt &= U^{-1} \int_{t_k}^{t_{k+1}} (\Sigma_{\delta(t)} - \mathcal{A}_{\delta(t)}) dt U \\ &= U^{-1} (\rho(\bar{\mathcal{A}}) I_N - \bar{\mathcal{A}}) U \\ &= \rho(\bar{\mathcal{A}}) I_N - \mathcal{J}_{\bar{\mathcal{A}}} \\ &= \begin{bmatrix} 0 & 0_{1 \times (N-1)} \\ 0_{(N-1) \times 1} & \rho(\bar{\mathcal{A}}) I_{N-1} - \mathcal{J}_{\bar{\mathcal{A}}_{N-1}} \end{bmatrix}. \end{aligned} \quad (\text{E5})$$

Compare (E4) with (E5), it is obvious that  $\int_{t_k}^{t_{k+1}} L_{\delta(t)}^* dt = \rho(\bar{\mathcal{A}}) I_{N-1} - \mathcal{J}_{\bar{\mathcal{A}}_{N-1}}$ . Let  $\Phi = \text{col}(\Phi_1, \Phi_{N-1})$ . Splitting dynamics (E3) gives

$$\dot{\Phi}_1 = -\mu_1 (l_{\delta(t)} \otimes I_p) \Phi_{N-1}, \quad (\text{E6a})$$

$$\dot{\Phi}_{N-1} = -\mu_1 \left( L_{\delta(t)}^* \otimes I_p \right) \Phi_{N-1}. \quad (\text{E6b})$$

Now we consider the average system of (E6b) within time interval  $[t_k, t_{k+1})$  as follows:

$$\begin{aligned} \dot{\bar{\Phi}}_{N-1} &= -\mu_1 \frac{\int_{t_k}^{t_{k+1}} \left( L_{\delta(t)}^* \otimes I_p \right) dt}{t_{k+1} - t_k} \bar{\Phi}_{N-1} \\ &= -\mu_1 \frac{\rho(\bar{\mathcal{A}}) I_{N-1} - \mathcal{J}_{\bar{\mathcal{A}}_{N-1}}}{t_{k+1} - t_k} \bar{\Phi}_{N-1}. \end{aligned} \quad (\text{E7})$$

Since  $\rho(\bar{\mathcal{A}})$  is the spectral radius of matrix  $\bar{\mathcal{A}}$ , we have that  $\forall i \geq 2$ ,  $\text{Re}(\rho(\bar{\mathcal{A}}) - \lambda_i(\bar{\mathcal{A}})) > 0$ . Thus, the average system (E7) is exponentially stable for any positive  $\mu_1$ . Then by Lemma 2, if  $T$  is small enough, the original system (E6b) is exponentially stable as well, i.e.  $\Phi_{N-1} \rightarrow 0$  exponentially as  $t \rightarrow \infty$ . Since  $\Phi = (U^{-1} \otimes I_p)S$ , we have

$$\lim_{t \rightarrow \infty} S(t) = \lim_{t \rightarrow \infty} [(U \otimes I_p) \text{col}(\Phi_1, 0_{(N-1)p \times p})] = \lim_{t \rightarrow \infty} (v_r \otimes \Phi_1).$$

From Assumption 1, we have that  $\mathcal{A}_{\delta(t)}$  is bounded and so is  $L_{\delta(t)}$ . Then with (E6a), where  $l_{\delta(t)} = u_l L_{\delta(t)} v_{N-1}$ , we have  $\dot{\Phi}_1 \rightarrow 0$  as  $t \rightarrow \infty$ . Hence,  $\Phi_1$  eventually converges to a constant matrix, denoted as  $S^*$ , and

$$\lim_{t \rightarrow \infty} S_i(t) = v_{r_i} S^*.$$

Therefore, ‘‘observer’’ (2a) achieves sign consensus. The proof is thus completed.

Reflect on the proof of Lemma 6, we have

$$S^* = \lim_{t \rightarrow \infty} \Phi_1 = \Phi_1(0) + \lim_{t \rightarrow \infty} \int_0^t -\mu_1 (l_{\delta(\tau)} \otimes I_p) \Phi_{N-1}(\tau) d\tau.$$

Since  $l_{\delta(t)}$  is bounded and  $\Phi_{N-1} \rightarrow 0$  exponentially as  $t \rightarrow \infty$ , there exist positive constants  $M$ ,  $a$  and  $b$  such that  $\|l_{\delta(t)}\| \leq M$  and  $\|\Phi_{N-1}\| \leq ae^{-bt}$ . Then we obtain

$$S^* \leq \Phi_1(0) + \frac{\mu_1 M a}{b}.$$

Denote the first row of  $U^{-1}$  as  $u^T = \text{col}(u_1, u_2, \dots, u_N)$ . With  $\Phi = (U^{-1} \otimes I_p)S$ , we have  $\Phi_1(0) = \sum_{i=1}^N u_i S_i(0)$ . We can see that  $S^*$  not only depends on the initial conditions of the ‘‘observer’’ (2a) and the topology of the graph, but also the nature of the ‘‘observer’’ itself.

Next, we show that ‘‘sign observer’’ (2b) can also reach sign consensus.

**Lemma 7.** Consider ‘‘sign observer’’ (2b). Under Assumption 1, if

$$\mu_1 > \frac{2\|S^*\|}{\rho(\bar{\mathcal{A}}) - \lambda_1},$$

where  $\lambda_1$  is the second largest real part of  $\bar{\mathcal{A}}$ 's eigenvalues, and there exist positive constants  $T$ ,  $S_M$ ,  $\omega$  and a symmetric positive definite matrix  $H$ , such that

$$\mu_2 > \frac{1 + T^2 S_M^2 \|H\|^2}{\omega},$$

then for arbitrary initial conditions  $\zeta_i(0)$ ,  $\zeta_i(t)$  achieves sign consensus,  $\forall i$ .

*Proof.* Introduce the transformation  $\hat{\zeta} = P(t)\zeta$ , where  $P(t) = e^{Qt}$  and  $Q = -I_N \otimes S^*$ . Take the time derivative of  $\hat{\zeta}$  as

$$\begin{aligned} \dot{\hat{\zeta}} &= Qe^{Qt}\zeta + e^{Qt}(S_d - \mu_2 L_{\delta(t)} \otimes I_p + I_N \otimes S^* - I_N \otimes S^*)\zeta \\ &= e^{Qt}(S_d - I_N \otimes S^*)e^{-Qt}\hat{\zeta} - \mu_2 e^{Qt}(L_{\delta(t)} \otimes I_p)e^{-Qt}\hat{\zeta} \\ &= e^{Qt}(S_d - I_N \otimes S^*)e^{-Qt}\hat{\zeta} - \mu_2 (L_{\delta(t)} \otimes I_p)\hat{\zeta}. \end{aligned}$$

From Lemma 6, we have  $S_i(t) \rightarrow S^*$  exponentially at the rate of  $\mu_1(\rho(\bar{\mathcal{A}}) - \lambda_1)$ . It is trivial to show that both  $\|e^{Qt}\|$  and  $\|e^{-Qt}\|$  are less than  $e^{\|S^*\|t}$ . Define  $\tilde{S}_d = e^{Qt}(S_d - I_N \otimes S^*)e^{-Qt} = \text{diag}(\tilde{S}_{d_1}, \dots, \tilde{S}_{d_N})$ . It can be verified that  $\tilde{S}_d \rightarrow 0$  exponentially as  $t \rightarrow \infty$  if  $\mu_1 > \frac{2\|S^*\|}{\rho(\bar{\mathcal{A}}) - \lambda_1}$ , where  $\lambda_1$  is the second largest real part of  $\bar{\mathcal{A}}$ 's eigenvalues.

Let  $e_{\hat{\zeta}} = (E \otimes I_p)\hat{\zeta}$ , where matrix  $E$  is defined as in (D3). Along with Lemma 3, we obtain

$$\begin{aligned} \dot{e}_{\hat{\zeta}} &= (E \otimes I_p)\tilde{S}_d\hat{\zeta} - \mu_2(EM_{\delta(t)}E \otimes I_p)\hat{\zeta} \\ &= (E \otimes I_p)\tilde{S}_d\hat{\zeta} - \mu_2(EM_{\delta(t)} \otimes I_p)e_{\hat{\zeta}}. \end{aligned} \quad (\text{E8})$$

Consider the Lyapunov function candidate  $V = e_{\hat{\zeta}}^T(H \otimes I_p)e_{\hat{\zeta}}$ , where  $H \in \mathbb{R}^{(N-1) \times (N-1)}$  is a symmetric positive definite matrix which will be specified later. It is obvious that this selection of  $V$  satisfies condition 1 in Lemma 1. Manipulating  $V$  as in condition 2 of Lemma 1 gives

$$\frac{\partial V}{\partial e_{\hat{\zeta}}}(e_{\hat{\zeta}}) \int_{t_k}^{t_{k+1}} \dot{e}_{\hat{\zeta}}(t) dt = 2e_{\hat{\zeta}}^T(H \otimes I_p) \int_{t_k}^{t_{k+1}} (E \otimes I_p)\tilde{S}_d\hat{\zeta} dt - 2\mu_2 e_{\hat{\zeta}}^T(H \otimes I_p) \left[ \int_{t_k}^{t_{k+1}} (EM_{\delta(t)} \otimes I_p) dt \right] e_{\hat{\zeta}}.$$

Let  $V_1 = 2e_\zeta^T (H \otimes I_p) \int_{t_k}^{t_k+1} (E \otimes I_p) \tilde{S}_d \hat{\zeta} dt$  and  $V_2 = -2\mu_2 e_\zeta^T (H \otimes I_p) \left[ \int_{t_k}^{t_k+1} (EM_{\delta(t)} \otimes I_p) dt \right] e_\zeta$ . Since  $\tilde{S}_d \rightarrow 0$  exponentially as  $t \rightarrow \infty$ , there exists  $S_M > 0$  such that  $\|\tilde{S}_d\| \leq S_M$ . Then

$$\begin{aligned} V_1 &\leq e_\zeta^T e_\zeta + (H \otimes I_p) \left[ \int_{t_k}^{t_k+1} (E \otimes I_p) \tilde{S}_d \hat{\zeta} dt \right]^T \left[ \int_{t_k}^{t_k+1} (E \otimes I_p) \tilde{S}_d \hat{\zeta} dt \right] (H \otimes I_p) \\ &\leq e_\zeta^T e_\zeta + S_M^2 \|H\|^2 \left( \int_{t_k}^{t_k+1} e_\zeta dt \right)^T \left( \int_{t_k}^{t_k+1} e_\zeta dt \right) \\ &= \left( 1 + T^2 S_M^2 \|H\|^2 \right) \|e_\zeta\|^2. \end{aligned}$$

Notice that  $\bar{L} = \int_{t_k}^{t_k+1} (\Sigma_{\delta(t)} - \mathcal{A}_{\delta(t)}) dt = \rho(\bar{\mathcal{A}}) I_N - \bar{\mathcal{A}}$ , and can be decomposed as  $\bar{L} = \int_{t_k}^{t_k+1} L_{\delta(t)} dt = \int_{t_k}^{t_k+1} M_{\delta(t)} E dt = \bar{M} E$ . Assumption 1 ensures that  $\bar{\mathcal{A}}$  is eventually positive. Then from Lemma 3, we know that  $\text{Re}(\lambda_i(E\bar{M})) > 0$  for all  $i$ ; thus,  $\int_{t_k}^{t_k+1} (EM_{\delta(t)} \otimes I_p) dt$  is Hurwitz and  $\exists H > 0$  such that

$$\left[ \int_{t_k}^{t_k+1} (EM_{\delta(t)} \otimes I_p) dt \right]^T (H \otimes I_p) + (H \otimes I_p) \left[ \int_{t_k}^{t_k+1} (EM_{\delta(t)} \otimes I_p) dt \right] \leq -w I_{(N-1)p \times (N-1)p},$$

for some positive scalar  $w$ , which allows  $V_2 \leq -\mu_2 w \|e_\zeta\|^2$ . Then we have  $\frac{\partial V}{\partial e_\zeta} (e_\zeta) \int_{t_k}^{t_k+1} \dot{e}_\zeta(t) dt \leq -w^* \|e_\zeta\|^2$  for some positive scalar  $w^*$  as long as  $\mu_2 > \frac{1+T^2 S_M^2 \|H\|^2}{w}$ , which satisfies condition 2 of Lemma 1. Thus,  $e_\zeta \rightarrow 0$  exponentially as  $t \rightarrow \infty$ .

Next, we study the boundedness of  $\hat{\zeta}$ . Notice that

$$\begin{aligned} (L_{\delta(t)} \otimes I_p) \hat{\zeta} &= (M_{\delta(t)} E \otimes I_p) \hat{\zeta} \\ &= (M_{\delta(t)} \otimes I_p) e_\zeta. \end{aligned}$$

Since we already have that  $e_\zeta \rightarrow 0$  exponentially as  $t \rightarrow \infty$ ,  $(L_{\delta(t)} \otimes I_p) \hat{\zeta} \rightarrow 0$  exponentially as  $t \rightarrow \infty$ . Also,  $\tilde{S}_d \rightarrow 0$  exponentially with  $\mu_1 > \frac{2\|S^*\|}{\rho(\bar{\mathcal{A}}) - \lambda_1}$ . Then, by Lemma 4,  $\hat{\zeta}$  eventually approaches to a bounded vector.

Now that  $e_\zeta$  vanishes, and  $\hat{\zeta}$  eventually converges to a bounded vector. There exists a bounded vector  $\hat{\zeta}^* \in \mathbb{R}^p$  such that  $\lim_{t \rightarrow \infty} \hat{\zeta} = v_r \otimes \hat{\zeta}^*$ . Thus, according to the definition of  $\hat{\zeta}$ , we have  $\lim_{t \rightarrow \infty} \zeta_i = v_{r_i} e^{S^* t} \hat{\zeta}^*$ . In other words, sign consensus of  $\zeta$  is achieved. The proof is thus completed.

## Appendix F Proof of Theorem 1

*Proof.* Consider (1) and (3), and let

$$\begin{aligned} \tilde{x}_i &= x_i - v_{r_i} \Pi_i \theta_i, & \tilde{u}_i &= u_i - \Gamma_i \theta, & e_i &= y_i - v_{r_i} \theta, \\ \epsilon_i &= \zeta_i - v_{r_i} \theta, & K_{\zeta_i} &= \frac{1}{v_{r_i}} \Gamma_i - K_i \Pi_i, & \tilde{K}_{\zeta_i}(t) &= K_{\zeta_i}(t) - K_{\zeta_i}. \end{aligned}$$

Straightforward computation gives

$$\begin{aligned} \dot{\tilde{x}}_i &= A_i x_i + B_i u_i - v_{r_i} \Pi_i S^* \theta \\ &= A_i (\tilde{x}_i + v_{r_i} \Pi_i \theta) + B_i (\tilde{u}_i + \Gamma_i \theta) - v_{r_i} \Pi_i S^* \theta \\ &= A_i \tilde{x}_i + B_i \tilde{u}_i, \end{aligned}$$

where the last equation utilizes the regulator equation (D5), and

$$\begin{aligned} \tilde{u}_i &= K_i x_i + K_{\zeta_i}(t) \zeta_i - \Gamma_i \theta \\ &= K_i (\tilde{x}_i + v_{r_i} \Pi_i \theta) + K_{\zeta_i}(t) (\epsilon_i + v_{r_i} \theta) - \Gamma_i \theta \\ &= K_i \tilde{x}_i + K_{\zeta_i}(t) \epsilon_i + (\Gamma_i - v_{r_i} K_{\zeta_i}) \theta + v_{r_i} K_{\zeta_i}(t) \theta - \Gamma_i \theta \\ &= K_i \tilde{x}_i + K_{\zeta_i}(t) \epsilon_i + v_{r_i} \tilde{K}_{\zeta_i}(t) \theta, \quad i = 1, \dots, N, \end{aligned}$$

which leads to

$$\begin{aligned} \dot{\tilde{x}}_i &= A_i \tilde{x}_i + B_i \left( K_i \tilde{x}_i + K_{\zeta_i}(t) \epsilon_i + v_{r_i} \tilde{K}_{\zeta_i}(t) \theta \right) \\ &= (A_i + B_i K_i) \tilde{x}_i + B_i K_{\zeta_i}(t) \epsilon_i + v_{r_i} B_i \tilde{K}_{\zeta_i}(t) \theta. \end{aligned} \tag{F1}$$

By Lemma 7 and the section *Virtual leader construction* in the main article, we have  $\epsilon_i \rightarrow 0$  as  $t \rightarrow \infty$  if  $\mu_1$  and  $\mu_2$  are large enough. Also, Lemma 5 enables  $\tilde{K}_{\zeta_i}(t)$  to vanish as  $t \rightarrow \infty$  if  $\mu_3$  is sufficiently large. With  $A_i + B_i K_i$  being Hurwitz, system (F1) is input-to-state stable with input  $B_i K_{\zeta_i}(t) \epsilon_i + v_{r_i} B_i \tilde{K}_{\zeta_i}(t) \theta$ . Thus,  $\tilde{x}_i(t) \rightarrow 0$  as  $t \rightarrow \infty$ , and the error

$$\begin{aligned} e_i &= C_i x_i - v_{r_i} \theta \\ &= C_i (\tilde{x}_i + v_{r_i} \Pi_i \theta) - v_{r_i} \theta \\ &= C_i \tilde{x}_i, \end{aligned}$$

decays to 0 as well. Thus,  $y_i \rightarrow v_{r_i} \theta$  as  $t \rightarrow \infty$ . Since  $v_r > 0$  by Proposition 1, along with Problem 1 we have

$$\begin{aligned} \lim_{t \rightarrow \infty} [\text{sgn}(y_{i_l}(t)) - \text{sgn}(\theta_l(t))] &= \lim_{t \rightarrow \infty} [\text{sgn}(v_{r_i} \theta_l(t)) - \text{sgn}(\theta_l(t))] \\ &= 0, \quad l \in L_1; \\ \lim_{t \rightarrow \infty} (y_{i_l}(t) - \theta_l(t)) &= \lim_{t \rightarrow \infty} (v_{r_i} \theta_l(t) - \theta_l(t)) \\ &= 0, \quad l \in L_2, \quad \forall i. \end{aligned}$$

Therefore, LOSC of MAS (1) is reached by control law (2), (D4) and (4). The proof is thus completed.

## Appendix G Proof of Theorem 2

*Proof.* Let  $\hat{x}_i = x_i - \xi_i$ . Taking the time derivative of  $\hat{x}_i$  gives

$$\begin{aligned}\dot{\hat{x}}_i &= A_i x_i + B_i u_i - A_i \xi_i - B_i u_i - L_i (y_i - C_i \xi_i) \\ &= (A_i - L_i C_i) \hat{x}_i, \quad i = 1, \dots, N.\end{aligned}\tag{G1}$$

Define  $\tilde{x}_i$  and  $\tilde{u}_i$  as in the development of Theorem 1. Then we have

$$\dot{\tilde{x}}_i = A_i \tilde{x}_i + B_i \tilde{u}_i,$$

and

$$\begin{aligned}\tilde{u}_i &= K_i \xi_i + K_{C_i} \zeta_i - \Gamma_i \theta \\ &= K_i (\tilde{x}_i + v_{r_i} \Pi_i \theta - \hat{x}_i) + K_{C_i}(t) (\epsilon_i + v_{r_i} \theta) - \Gamma_i \theta \\ &= K_i \tilde{x}_i - K_i \hat{x}_i + K_{C_i}(t) \epsilon_i + v_{r_i} \tilde{K}_{C_i}(t) \theta,\end{aligned}$$

which lead to

$$\dot{\tilde{x}}_i = (A_i + B_i K_i) \tilde{x}_i - B_i K_i \hat{x}_i + B_i K_{C_i}(t) \epsilon_i + v_{r_i} B_i \tilde{K}_{C_i}(t) \theta.\tag{G2}$$

With  $A_i - L_i C_i$  being Hurwitz,  $\hat{x}_i \rightarrow 0$  as  $t \rightarrow \infty$ . Following similar development as in the proof of Theorem 1, we can show that  $\tilde{x}_i$  vanishes, and further  $\epsilon_i$  vanishes. Since  $v_r > 0$  by Proposition 1, along with Problem 1 we have

$$\begin{aligned}\lim_{t \rightarrow \infty} [\text{sgn}(y_{i_l}(t)) - \text{sgn}(\theta_l(t))] &= \lim_{t \rightarrow \infty} [\text{sgn}(v_{r_i} \theta_l(t)) - \text{sgn}(\theta_l(t))] \\ &= 0, \quad l \in L_1 \\ \lim_{t \rightarrow \infty} (y_{i_l}(t) - \theta_l(t)) &= \lim_{t \rightarrow \infty} (v_{r_i} \theta_l(t) - \theta_l(t)) \\ &= 0, \quad l \in L_2, \quad \forall i\end{aligned}$$

Therefore, LOSC of MAS (1) is reached by control law (2), (D4) and (5). The proof is thus completed.

## Appendix H Simulation example

Consider a MAS with 6 agents, and the dynamics (1) of each agent takes the following values:

$$A_i = \begin{bmatrix} -0.08 & 16.05 \\ -31.61 & 0.06 \end{bmatrix}, B_i = \begin{bmatrix} 1 \\ 3 \end{bmatrix}, C_i = \begin{bmatrix} 0 & 1 \\ 1 & 0 \end{bmatrix}, \quad i = 1, 2, 3;\tag{H1a}$$

$$A_i = \begin{bmatrix} 0.06 & -31.61 \\ 16.05 & -0.08 \end{bmatrix}, B_i = \begin{bmatrix} 2 \\ 4 \end{bmatrix}, C_i = \begin{bmatrix} 1 & 0 \\ 0 & 1 \end{bmatrix}, \quad i = 4, 5, 6.\tag{H1b}$$

It can be verified that all  $(A_i, B_i, C_i)$  are both controllable and observable. ‘‘Observer’’ (2a) are with the following initial conditions:

$$\begin{aligned}S_1(0) &= \begin{bmatrix} 0 & 3 \\ -2 & 0 \end{bmatrix}, S_2(0) = \begin{bmatrix} -0.01 & 5 \\ -3 & 0.01 \end{bmatrix}, S_3(0) = \begin{bmatrix} -0.01 & 4 \\ -2 & 0.02 \end{bmatrix}, \\ S_4(0) &= \begin{bmatrix} -0.01 & 4 \\ -4 & 0.01 \end{bmatrix}, S_5(0) = \begin{bmatrix} -0.01 & 6 \\ -1 & 0.02 \end{bmatrix}, S_6(0) = \begin{bmatrix} -0.02 & 5 \\ -2.5 & 0.01 \end{bmatrix}.\end{aligned}$$

The communication graphs of the MAS are shown in Figs.H1-H4, and the switching signal is described as:

$$\delta(t) = \begin{cases} 1, & kT \leq t < kT + 7.3 \times 10^{-4}, \\ 2, & kT + 7.3 \times 10^{-4} \leq t < kT + 1.2 \times 10^{-3}, \\ 3, & kT + 1.2 \times 10^{-3} \leq t < kT + 1.5 \times 10^{-3}, \\ 4, & kT + 1.5 \times 10^{-3} \leq t < (k+1)T, \end{cases}$$

where  $k = 0, 1, 2, \dots$  and  $T = 2.1 \times 10^{-3}$  s. By (D2), we choose  $T$  small enough, which allows us to choose  $\alpha^* < 1$ , and it is straightforward to show that the selected switching graph satisfies Assumption 1. According to Lemma 7 and Lemma 5, let  $\mu_1 = 1000$ ,  $\mu_2 = 100$  and  $\mu_3 = 1000$ . The following two subsections present the simulation results of the state feedback control case and the output feedback control case, respectively.

### Appendix H.1 State feedback control case

Let  $K_i$  be the following values such that  $A_i + B_i K_i$  is Hurwitz:

$$\begin{aligned}K_i &= \begin{bmatrix} -0.11 & -9.96 \end{bmatrix}, \quad \text{for } i = 1, 2, 3; \\ K_i &= \begin{bmatrix} -3.84 & -5.58 \end{bmatrix}, \quad \text{for } i = 4, 5, 6.\end{aligned}$$

The output signals of the MAS are plotted in Fig.H5 and Fig.H6. The figures show that LOSC is reached by the designed state feedback controller.

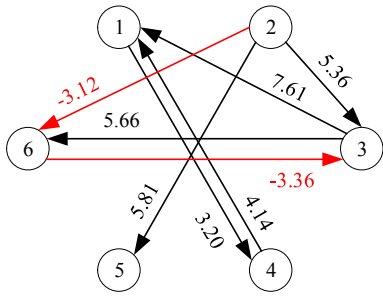


Figure H1 Signed graph  $\mathcal{G}(\mathcal{A}_1)$

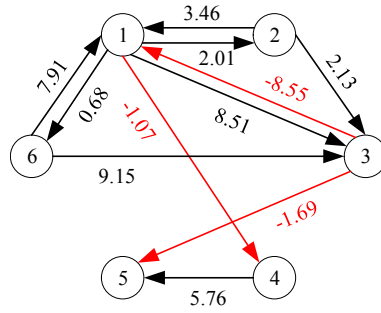


Figure H2 Signed graph  $\mathcal{G}(\mathcal{A}_2)$

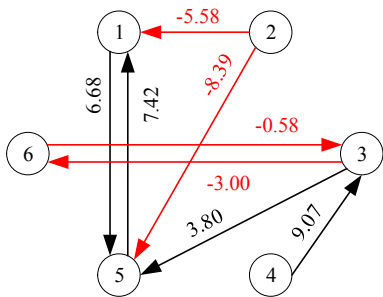


Figure H3 Signed graph  $\mathcal{G}(\mathcal{A}_3)$

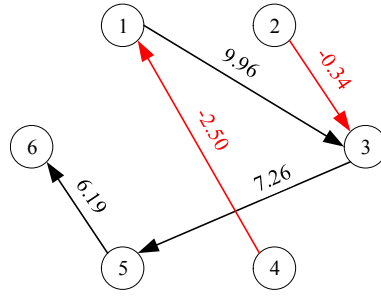


Figure H4 Signed graph  $\mathcal{G}(\mathcal{A}_4)$

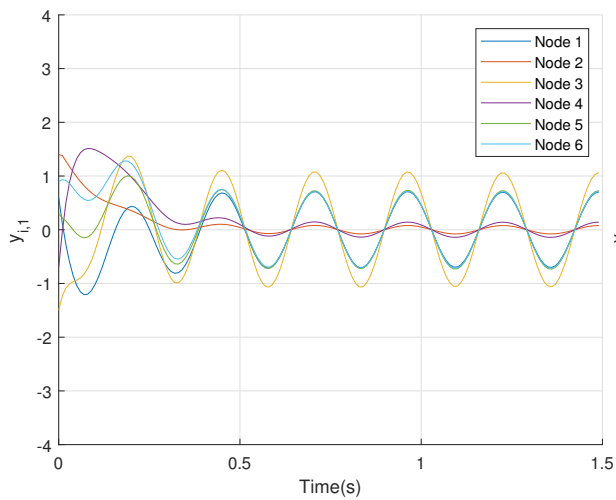


Figure H5 Output trajectories  $y_{i,1}$  for state feed-back control case

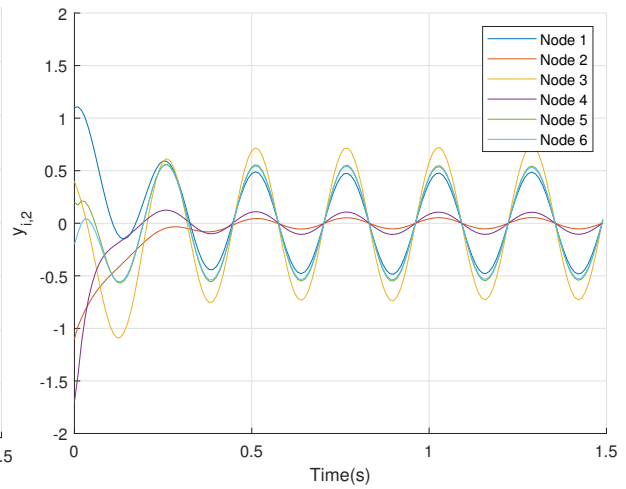
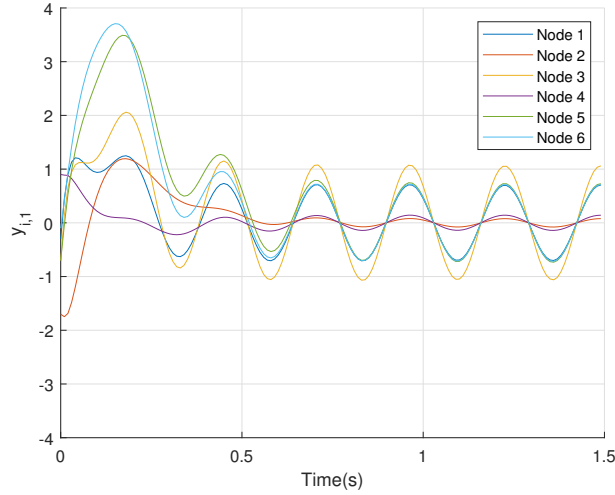
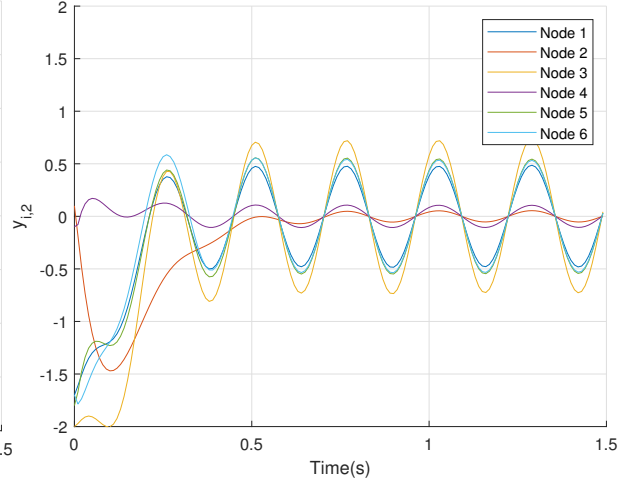


Figure H6 Output trajectories  $y_{i,2}$  for state feed-back control case





**Figure H7** Output trajectories  $y_{i,1}$  for output feedback control case



**Figure H8** Output trajectories  $y_{i,2}$  for output feedback control case

## Appendix H.2 Output feedback control case

Choose  $K_i$  as in the state feedback control case, and  $L_i$  takes the following values:

$$L_i = \begin{bmatrix} 16.05 & 9.92 \\ 20.06 & -31.61 \end{bmatrix}, \text{ for } i = 1, 2, 3;$$

$$L_i = \begin{bmatrix} 10.06 & -31.61 \\ 16.05 & 19.92 \end{bmatrix}, \text{ for } i = 4, 5, 6.$$

The above selection of  $K_i$  and  $L_i$  ensures that  $A_i + B_i K_i$  and  $A_i - L_i C_i$  are Hurwitz for all  $i$ . The output signals of the MAS are plotted in Fig.H7 and Fig.H8. The presented figures illustrate that LOSC is reached by the designed output feedback controller.

### References

- 1 Yan L, Chen W, Li C, et al. Consensus-based distributed power control in power grids. *Science China Information Sciences*, 2020, 63: 149202
- 2 Wang Y, Guo G, Yue W. Queue estimation for isolated signalized intersections in intelligent vehicle-infrastructure cooperation systems. *Science China Information Sciences*, 2021, 64: 149203
- 3 Guo K, Li X, Xie L. Simultaneous cooperative relative localization and distributed formation control for multiple UAVs. *Science China Information Sciences*, 2020, 63: 119201
- 4 Ren W, Beard R. *Distributed Consensus in Multi-vehicle Cooperative Control: Theory and Application*. London, UK: Springer-Verlag, 2008
- 5 Lewis FL, Zhang H, Hengster-Movric K, et al. *Cooperative Control of Multi-agent Systems: Optimal and Adaptive Design Approaches*. London, UK: Springer-Verlag, 2014
- 6 Yu W, Wang H, Hong H, et al. Distributed cooperative anti-disturbance control of multi-agent systems: An overview. *Science China Information Sciences*, 2017, 60: 110202
- 7 Berman A, Plemmons RJ. *Non-negative Matrices in the Mathematical Sciences*. Philadelphia, PA: SIAM, 1994
- 8 Liu Q, He X, Fang H. Asymptotic properties of distributed social sampling algorithm. *Science China Information Sciences*, 2020, 63: 112202
- 9 Stavroglou SK, Pantelous AA, Stanley HE, et al. Hidden interactions in financial markets. *Proceedings of the National Academy of Sciences*, 2019, 116: 10646-10651
- 10 Saberi M, Khosrowabadi R, Khatibi A, et al. Topological impact of negative links on the stability of resting-state brain network. *Scientific Reports*, 2021, 11: 1-4
- 11 Altafani C. Consensus problems on networks with antagonistic interactions. *IEEE Transactions on Automatic Control*, 2012, 58: 935-946
- 12 Harary F. On the notion of balance of a signed graph. *Michigan Mathematical Journal*, 1953, 2:143-146
- 13 Zhang H, Chen J. Bipartite consensus of multi-agent systems over signed graphs: State feedback and output feedback control approaches. *International Journal of Robust and Nonlinear Control*, 2017, 27: 3-14
- 14 Valcher ME, Misra P. On the consensus and bipartite consensus in high-order multi-agent dynamical systems with antagonistic interactions. *Systems & Control Letters*, 2014, 66: 94-103
- 15 Pan L, Shao H, Xi Y, et al. Bipartite consensus problem on matrix-valued weighted directed networks. *Science China Information Sciences*, 2021, 64: 149204
- 16 Noutsos D. On Perron-Frobenius property of matrices having some negative entries. *Linear Algebra and Its Applications*, 2006, 412: 132-153
- 17 Naqvi SC, McDonald JJ. The combinatorial structure of eventually non-negative matrices. *Electronic Journal of Linear Algebra*, 2002, 9: 255-269
- 18 Altafani C, Lini G. Predictable dynamics of opinion forming for networks with antagonistic interactions. *IEEE Transactions on Automatic Control*, 2015, 60: 342-357

- 19 Jiang Y, Zhang H, Chen J. Sign-consensus of linear multi-agent systems over signed directed graphs. *IEEE Transactions on Industrial Electronics*, 2016, 64: 5075-5083
- 20 Zhai S, Zheng WX. Dynamic behavior for social networks with state-dependent susceptibility and antagonistic interactions. *Automatica*, 2021, 129:109652
- 21 Sun Z, Zhang H, Lewis FL. Output sign-consensus of heterogeneous multi-agent systems over fixed and switching signed graphs: An observer-based approach. *International Journal of Robust and Nonlinear Control*, 2021, 31: 5849-5864
- 22 Jiang Y, Zhang H, Chen J. Sign-consensus over cooperative-antagonistic networks with switching topologies. *International Journal of Robust and Nonlinear Control*, 2018, 28: 6146-6162
- 23 Jiang H, Zhang H. Output sign-consensus of heterogeneous multiagent systems over fixed and switching signed graphs. *International Journal of Robust and Nonlinear Control*, 2020, 30: 1938-1955
- 24 Meng M, Xiao G, Li B. Adaptive consensus for heterogeneous multi-agent systems under sensor and actuator attacks. *Automatica*, 2020, 122:109242
- 25 Deng C, Zhang D, Feng G. Resilient practical cooperative output regulation for MASs with unknown switching exosystem dynamics under DoS attacks. *Automatica*, 2022, 139:110172
- 26 Bode NW, Wood AJ, Franks DW. Social networks improve leaderless group navigation by facilitating long-distance communication. *Current Zoology*, 2012, 58: 329-341
- 27 Wang S, Zhang H, Baldi S, Zhong R. Leaderless consensus of heterogeneous multiple Euler-Lagrange systems with unknown disturbance. *IEEE Transactions on Automatic Control*, 2022, 68: 2399-2406
- 28 Meng Y, Wang S, Zhang H. Leaderless output sign consensus of heterogeneous multi-agent systems over signed graphs. *International Journal of Robust and Nonlinear Control*, 2022, 32:10125-10138
- 29 Rand DG, Arbesman S, Christakis NA. Dynamic social networks promote cooperation in experiments with humans. *Proceedings of the National Academy of Sciences*, 2011, 108: 19193-19198
- 30 Aeyels D, Peuteman J. On exponential stability of nonlinear time-varying differential equations. *Automatica*, 1999, 35: 1091-1101